Electronic Supplementary Material (ESI) for Physical Chemistry Chemical Physics.
This journal is © the Owner Societies 2014

Supporting Information

C_2H_4 purity

The purity of the ethene feed was checked by means of GC-MS analysis (Agilent, GC 6890 with MSD 5973, separation column: HP-5MS 19091S-433) with special attention to other unsaturated compounds. A flow of $[C_2H_4] = 5.0 \cdot 10^{13}$ molecule cm^{-3} from a gas mixing unit in air at 1 bar was pumped continuously through a heated GC-loop coupled with a pre-focusing device where the gas sample from the GC-loop was flushed through an uncoated, deactivated fused silica capillary (0.32 mm i.d.) and trapped at liquid N_2 temperature. After flash heating, the substances were directly injected at the separation column. This approach allows the detection of compounds with concentrations down to 10^9 molecule cm^{-3}.[S1] Figure S1 shows the total ion chromatogram in the range 35 - 150 amu. Ethene is not detectable under these conditions, but all other unsaturated impurities like propene, the butenes, etc. Beside the system-permanent impurities acetone and benzene, no other compounds were observed. A conservative estimated yields an upper limit of unsaturated impurities of $5 \cdot 10^9$ molecule cm^{-3}, i.e. $1/10^4$ of the concentration of ethene.

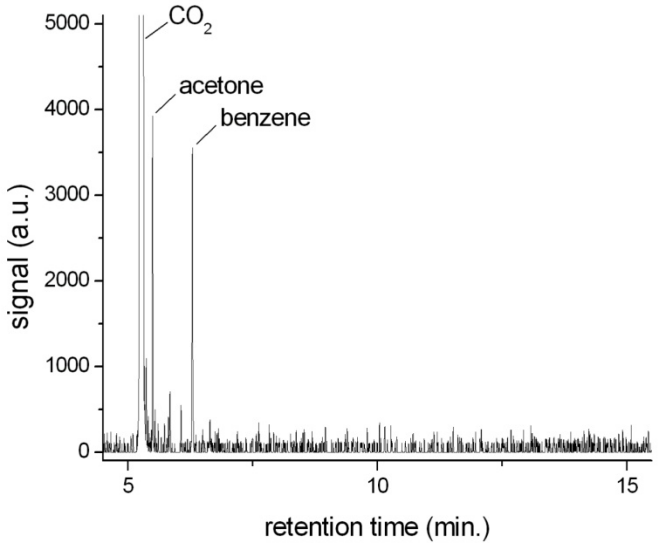

Fig.S1: Gas chromatogram of an ethene sample ($5.0 \cdot 10^{13}$ molecule cm^{-3}) diluted in air.

Modelling of the reaction system

Modelling of the reaction system at RH = 0% has been performed in order to assess the importance of different steps for the consumption of CH_2OO under the chosen experimental conditions. For simplicity, the OH radical chemistry was omitted because all runs for the CH_2OO kinetics were conducted in presence of an OH radical scavenger.

$O_3 + C_2H_4 \rightarrow 0.4 \cdot CH_2OO + CH_2O + ... ;\ 1.58 \cdot 10^{-18}$ cm^3 molecule^{-1} s^{-1} (S1)

$CH_2OO + SO_2 \rightarrow CH_2O + SO_3(H_2SO_4) ;\ 3.9 \cdot 10^{-11}$ or $3.9 \cdot 10^{-12}$ cm^3 molecule^{-1} s^{-1} (S2)

$CH_2OO \rightarrow$ dioxirane, OH, ... ; 100 or 0.3 s^{-1} (S3)

$CH_2OO \rightarrow$ wall ; 0.034 s^{-1} (S4)

$CH_2OO + CH_2OO \rightarrow$ products ; $2 \cdot 10^{-10}$ cm^3 molecule^{-1} s^{-1} (S5)

$CH_2OO + CH_2O \rightarrow$ products ; $1 \cdot 10^{-12}$ cm^3 molecule^{-1} s^{-1} (S6)

$CH_2OO + H_2SO_4 \rightarrow$ products ; $5 \cdot 10^{-12}$ cm^3 molecule^{-1} s^{-1} (S7)

The rate coefficient k_{S1} was taken from ref.S2, the CH_2OO formation yield of 0.4 for reaction (S1) from literature data and as a result of this study (see main text) and the CH_2O formation yield of unity from ref.S3. For k_{S2} the value by Welz et al.[S4] or one-tenth of that was used. Immediate H_2SO_4 formation from SO_3 in the RH range of 2 - 50% is assumed. For k_{S3} the data by Welz et al.[S4] (100 s^{-1} representing probably an upper limit) or Olzmann et al.[S5] (0.3 s^{-1}) was taken. The first-order rate coefficient for the diffusion-limited wall loss was estimated according $k_{S4} = 3.65 \cdot D/r^2$, D = diffusion coefficient of CH_2OO and r stands for the tube radius. As the diffusion coefficient a value of 0.15 cm^2 s^{-1} was adopted from experimental data for H_2O_2 [S6] resulting in $k_{S4} = 0.034$ s^{-1}. The rate coefficient k_{S5} was taken from literature[S7] and for k_{S6} a value obtained for $CH_2OO + CH_3CHO$[S8] was applied. The rate coefficient k_{S7} was taken from literature[S9] Initial conditions are: $[O_3] = 2.2 \cdot 10^{11}$, $[C_2H_4] = 1.5 \cdot 10^{13}$ and $[SO_2] = 1 \cdot 10^{12}$ molecule cm^{-3}, t = 39.5s.

Table S1: Result from modelling, pathways (S1) – (S6)

k_{S2} (cm^3 $molecule^{-1}$ s^{-1})	$3.9 \cdot 10^{-11}$	$3.9 \cdot 10^{-11}$	$3.9 \cdot 10^{-12}$
k_{S3} (s^{-1})	100	0.3	0.3
steady state [CH_2OO] (molecule cm^{-3})	$1.5 \cdot 10^{4}$	$5.3 \cdot 10^{4}$	$4.9 \cdot 10^{5}$
CH_2OO fraction reacting via			
path (S2)	0.28	0.99	0.92
path (S3)	0.72	$7.6 \cdot 10^{-3}$	0.07
path (S4)	$2.4 \cdot 10^{-4}$	$8.6 \cdot 10^{-4}$	$8.0 \cdot 10^{-3}$
path (S5)	$2.1 \cdot 10^{-8}$	$2.7 \cdot 10^{-7}$	$2.3 \cdot 10^{-5}$
path (S6)	$7.4 \cdot 10^{-7}$	$2.6 \cdot 10^{-6}$	$2.4 \cdot 10^{-5}$
path (S7)	$4.2 \cdot 10^{-7}$	$5.2 \cdot 10^{-6}$	$4.4 \cdot 10^{-5}$
H_2SO_4 fraction reacting via path (S7)	$1.5 \cdot 10^{-6}$	$5.2 \cdot 10^{-6}$	$4.8 \cdot 10^{-5}$

The CH_2OO fraction reacting in the self reaction via path (S5), in the reaction with CH_2O via path (S6) and with H_2SO_4 via path (S7) is in each case smaller than 10^{-4} (0.01 %) even for the lower rate coefficient k_{S2} and the lower value for k_{S3} (and low [SO_2] = 10^{12} molecule cm^{-3}). The diffusion-limited wall loss accounts for less than 1 % of CH_2OO consumption. The importance of pathways (S4) – (S6) is further pushed back for rising SO_2 concentrations and in the presence of water vapour. The steady state CH_2OO concentrations in these scenarios are in the range 10^4 - $5 \cdot 10^5$ molecule cm^{-3} and become lower with increasing SO_2 concentrations and increasing water vapour content. The H_2SO_4 fraction reacting with CH_2OO is also very small and cannot influence the data analysis.

Prompt OH radical formation

For high SO_2 concentrations (CH_2OO titration by SO_2), the measurements in absence of C_3H_8 showed some higher H_2SO_4 concentrations compared with the conditions in presence of C_3H_8 for OH radical scavenging, see Fig.2a. The additional H_2SO_4 is attributed to prompt OH radicals (y_1) reacting with SO_2 (~ 10^{14} molecule cm^{-3}) in competition with the reaction with C_2H_4 ($1.5 \cdot 10^{13}$ molecule cm^{-3}).

$$OH + SO_2 \rightarrow ... \rightarrow H_2SO_4 \qquad (S7)$$

$$OH + C_2H_4 \rightarrow \text{products} \qquad (S8)$$

The concentration of formed OH is:

$$[OH] = [H_2SO_4] \cdot (1 + \frac{k_{S8}[C_2H_4]}{k_{S7}[SO_2]}) \qquad (SI)$$

Rearrangement yields:

$$[H_2SO_4] = [OH] \cdot 1/(1 + \frac{k_{S8}[C_2H_4]}{k_{S7}[SO_2]}) \qquad (SII)$$

In Fig.S2 the data for the additional $[H_2SO_4]$ are plotted according to equation (SII) for different RH. The slope through the origin yields total [OH] = $(1.19 \pm 0.05) \cdot 10^7$ molecule cm^{-3}. The amount of reacted $[C_2H_4] = k_4[C_2H_4][O_3] \cdot t$ was $2.06 \cdot 10^8$ molecule cm^{-3} yielding a prompt OH radical yield y_1 = 0.06 ± 0.03. The error includes the uncertainty of H_2SO_4 calibration.

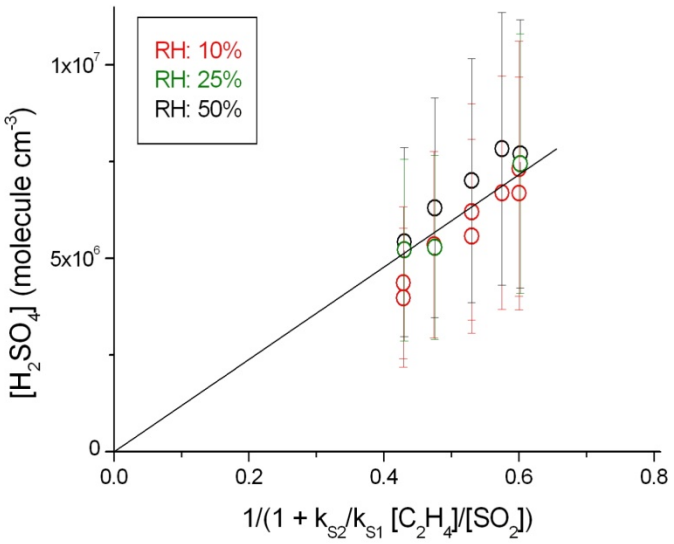

Fig.S2: Additional $[H_2SO_4]$ for different RH plotted according to equation (SII). Error bars represent the uncertainty of the H_2SO_4 measurement.

Supporting references:

S1 T. Berndt and O. Böge, *Phys. Chem. Chem. Phys.,* 2006, **8**, 1205.

S2 R. Atkinson, D. L. Baulch, R. A. Cox, R. F. Hampson, Jr., J. A. Kerr, M. J. Rossi and J. Troe, *J. Phys. Chem. Ref. Data*, 1997, **26**, 521.

S3 E. Grosjean and D. Grosjean, *Enviro. Sci. Technol.*, 1996, **30**, 2036.

S4 O. Welz, J. D. Savee, D. L. Osborn, S. S. Vasu, C. J. Percival, D. E. Shallcross and C. A. Taatjes, *Science*, 2012, **335**, 204.

S5 M. Olzmann, E. Kraka, D. Cremer, R. Gutbrot and S. Andersson, *J. Phys. Chem. A*, 1997, **101**, 9421.

S6 A. V. Ivanov, S. Trakhtenberg, A. K. Bertram, Y. M. Gershenzon and M. J. Molina, *J. Phys. Chem. A*, 2007, **111**, 1632.

S7 Y.-T. Su, H.-Y. Lin, R. Putikam, H. Matsui, M. C. Lin and Y.-P. Lee, *Nature Chem.*, 2014, doi: 10.1038/NCHEM.1890.

S8 C. A. Taatjes, O. Welz, A. J. Eskola, J. D. Savee, D. L. Osborn, E. P. F. Lee, J. M. Dyke, D. K. W. Mok, D. E. Shallcross and C. J. Percival, *Phys. Chem. Chem. Phys.*, 2012, **14**, 10391.

S9 L. Vereecken, H. Harder and A. Novelli, *Phys. Chem. Chem. Phys.*, 2012, **14**, 14682.